GeoVirtual 2020 September 14-16
Resilience and Innovation

Estimation of Stability of an Unsupported Deep Vertical Cut in Clay

Geeshpati Yanamandra & Won Taek Oh
Department of Civil Engineering – University of New Brunswick, Fredericton, New Brunswick, Canada

ABSTRACT
Finite element analysis was performed to simulate the excavation of an unsupported deep vertical cut (depth = 9.75 m) in clay at Welland, Ontario (Kwan 1971). For this, SIGMA/W and SLOPE/W (GeoStudio 2019 R2) were used to simulate staged excavation and to estimate its stability, respectively. To maintain the consistency of obtained results with field conditions, the simulated excavation followed the same timeline as field excavation. There was good agreement between the measured post excavation pore-water pressure contours obtained from installed field instruments with those from the numerical modelling. The numerical analysis results also showed that the failure in the cut was attributed to a tension crack, which is consistent with field observations.

RÉSUMÉ
Une analyse par éléments finis a été effectuée pour simuler l'excavation d'une coupe verticale profonde non soutenue (profondeur = 9,75 m) dans l'argile à Welland, Ontario (Kwan 1971). Pour cela, SIGMA / W et SLOPE / W (GeoStudio 2019 R2) ont été utilisés pour simuler l'excavation par étapes et pour estimer sa stabilité, respectivement. Pour maintenir la cohérence des résultats obtenus avec les conditions du terrain, l'excavation simulée a suivi la même chronologie que l'excavation sur le terrain. Il y avait un bon accord entre les contours de pression interstitielle mesurés après l'excavation obtenus à partir des instruments de terrain installés avec ceux de la modélisation numérique. Les résultats de l'analyse numérique ont également montré que la rupture de la coupe était attribuée à une fissure de tension, ce qui est cohérent avec les observations sur le terrain.

1 INTRODUCTION

Excavation of unsupported cuts in soil is a common practice in wide range of engineering projects. The stability of unsupported cuts throughout this activity is governed by the factors such as soil type, drainage condition, tension crack, and ground water table level.

Stability of unsupported cuts can be estimated extending either effective or total stress approaches. Figure 1 presents the variation of load, shear stress, pore pressure, strength, and factor of safety at point A on a slip surface due to excavation in saturated clay. Excavation causes decrease in mean total stress at a local point. This leads to decrease in pore-water pressure and drop in ground water table. However, rapid expanding or sucking in pore-water from the unaffected areas do not take place due to the viscous resistance to pore-water flow. During this period, undrained condition is achieved in the soil and effective stress (i.e. shear strength) remains constant; however, factor of safety decreases due to the increase in shear stress. With time, pore-water flows from the areas of higher pore-water pressure to those of lower pore-water pressure. This increases soil volume (i.e. swelling) and softens soil structure. Therefore, factor of safety further decreases under drained condition during this period. Total stress approach is required to analyze the stability of unsupported cuts before the redistribution of pore-water pressure initiates. The duration of undrained condition during excavation process varies depending on soil type (National Bureau of Standards 1988, Irvine and Smith 1983, Leroueil et al. 1990). The total stress approach (i.e. short-term condition, $\phi_u = 0$ analysis) is required to analyze the stability of unsupported cuts until the completion of excavation, and the effective stress approach (i.e. long-term condition) is required thereafter. Banerjee et al. (1988) concluded that dissipation of the excess negative pore-water pressure starts immediately after excavation, which justifies the use of effective stress approach (Lambe and Turner 1970, Kwan 1971, DiBagio and Roti 1972, Dysli and Fontana 1982) in analyzing the stability of unsupported cuts.

In the present study, a series of numerical analyses were carried out to estimate the stability of unsupported deep vertical cut in clay (Kwan 1971) extending the effective stress approach. Geotechnical modeling software, SIMGA/W and SLOPE/W (GeoStudio 2019 R2, GeoSlope Int. Ltd.) were used to simulate the excavation and redistribution of pore-water pressure and to conduct stability analysis, respectively. The numerical analysis results also showed that the failure in the unsupported vertical cut was attributed to a tension crack, which is consistent with field observations.

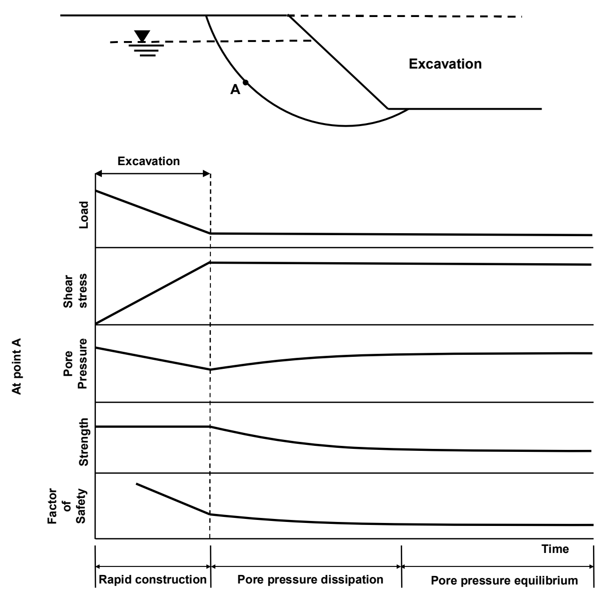

Figure 1. Variation of load, stress, pore pressure, strength, and factor of safety at point A due to excavation in saturated clay (modified after Bishop and Bjerrum 1960)

2 MODIFIED EFFECTIVE AND TOTAL STRESS APPRAOCHS

As mentioned earlier, shear strength of saturated soil can be estimated using either effective or total stress approach. Similar approaches can be used to estimate the shear strength of unsaturated soil extending the conventional effective or total stress approach. For unsaturated coarse-grained soil, it is reasonable to estimate the shear strength using the effective shear strength parameters (i.e. c' and ϕ' in Eq. [1] and ϕ^b, where ϕ^b = rate of shear strength increment due to matric suction) assuming both pore-air and pore-water are under drained condition during shearing stage. This approach is denoted as the modified effective stress approach. On the other hand, there are uncertainties in estimating the shear strength of unsaturated fine-grained soil due to the uncertainties of drainage conditions of pore-air and pore-water. In this case, shear strength can be estimated extending ϕ_u = 0 approach by including the contribution of matric suction in total cohesion (i.e. modified total stress approach). Eq. [1] (Vanapalli et al. 1996) and Eq. [2] (Oh and Vanapalli 2018) are the models developed based on the modified effective and modified total stress approach, respectively to estimate the variation of shear strength of soil with respect to matric suction.

$$\tau_{unsat} = c' + (\sigma_n - u_a)\tan\phi' + (u_a - u_w)\left(\frac{\theta - \theta_r}{\theta_s - \theta_r}\right)\tan\phi' \quad [1]$$

where, τ_{unsat} is shear strength of unsaturated soil under drained condition, c' is effective cohesion, ($\sigma_n - u_a$) is net normal stress, σ_n is normal stress, ϕ' is effective internal friction angle, (u_a -u_w) matric suction, u_a is pore-air pressure, u_w is pore-water pressure, θ is volumetric water content (subscript s is saturated condition and r is residual condition)

$$c_{u(unsat)} = c_{u(sat)}\left\{1 + \frac{\left[(u_a - u_w)/P_a\right](S)^{\zeta}}{\xi}\right\} \quad [2]$$

where, $c_{u(unsat)}$ is shear strength of unsaturated soil under undrained condition, $c_{u(sat)}$ is shear strength of saturated soil under undrained condition, ζ and ξ are fitting parameters, and P_a is atmospheric pressure (i.e. 101.3 kPa)

GeoStudio (2019 R2) adopts Eq. [1] to conduct stability analysis (i.e. modified effective stress approach). In case of undrained stability analysis, the undrained shear strength values need to be manually assigned to the elements based on the redistribution of pore-water pressure due to excavation. In the present study, the modified effective stress approach (Eq. [1]) was used to estimate the stability of unsupported deep vertical cut in clay.

3 DESCRIPTION OF FIELD EXCAVATION

Kwan (1971) investigated the behavior of an unsupported deep vertical cut and an inclined slope excavated in clay. Test excavation pits were made in Haldimand clay for realignment of southern half of Welland canal at Welland, Ontario. Excavation of test pits were proposed to be 15 m deep with the measurements of pore-water pressures and surface deformation. Proposed excavation mainly consisted of two stages:

Stage 1: Removal of top overburden desiccated clay to a depth of 5.2 m, sloped at 1:3 and with a berm of 6.1 m.

Stage 2: Excavating a 9.75 m unsupported vertical cut on one side and a 1:1 slope on the other.

To eliminate end effects, two vertical trenches were excavated at the ends, which limited the length of slope to 15.2 m.

Staged excavation was carried out for 27 days till the occurrence of failure. Timeline of the excavation is detailed in Figure 2. Multiple piezometers were installed after removal of top sediment and pressure head readings were taken for 12 days after removal.

Excavation profile and location of piezometers are shown in Figure 3. The pore-water pressures were dropped significantly in the areas located within a distance of 24.2 m from the unsupported vertical cut during the removal of top sediment layer and vertical excavation.

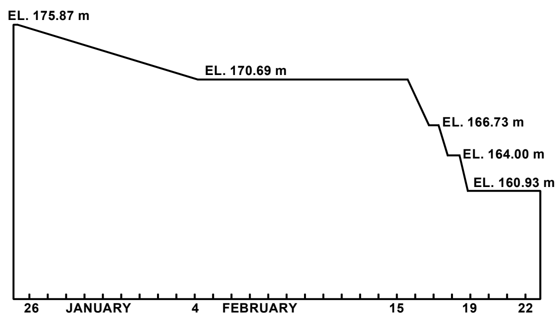

Figure 2. Timeline of excavation (after Kwan 1971)

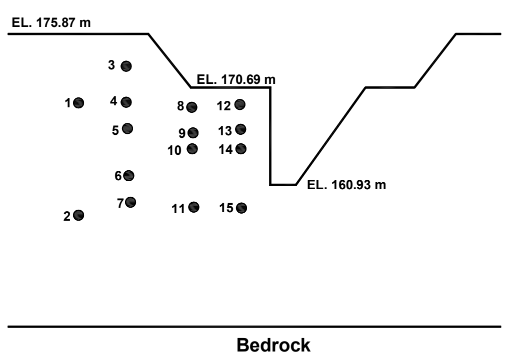

Figure 3. Excavation profile and location of piezometers (after Kwan 1971)

During the entire excavation period, low overall precipitation was recorded in the range of 0.25 mm to 10 mm. Hence, the precipitation event was not taken into account in the numerical analysis. The minimum temperature recorded was -25 °C; however, it rarely dropped below -18 °C. Kwan (1971) conducted a stability analysis of the unsupported vertical cut using both effective and total stress approaches. Later, Banerjee et al. (1988) carried out finite element analysis to estimate stability of the same unsupported vertical cut using the data available in Kwan (1971). However, the influence of matric suction on the shear strength of the soils was not taken into account in either study.

The reason for failure was due to the formation of a tension crack at the berm. Two tension cracks appeared after the completion of unsupported vertical cut. The identified potential slip surface due to the formation of the first tension crack was estimated to be at 6.4 m from the crest (Figure 4). However, the unsupported vertical cut unexpectedly failed along a new slip surface due to formation of the second tension crack at 2.43 m from the crest (Figure 5).

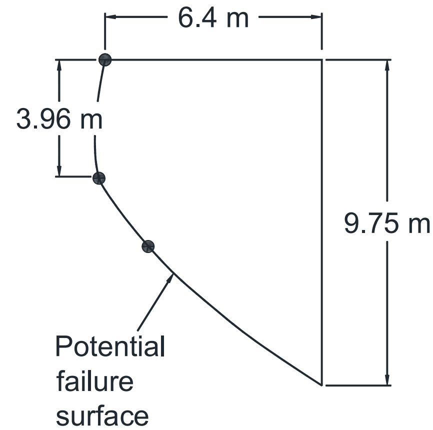

Figure 4. Identified potential slip surface with the first tension crack (after Kwan 1971)

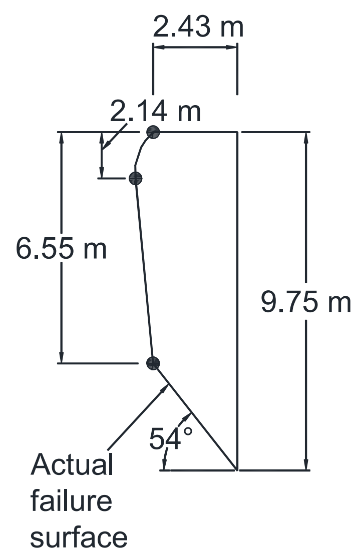

Figure 5. Actual slip surfaces with the second tension crack that led to the failure of unsupported vertical cut (after Kwan 1971)

Kwan (1971) performed total stress analysis to evaluate the stability of unsupported vertical cut using undrained shear strength. Undrained shear strength was back calculated considering different scenarios. For simplicity, the stratum was assumed to be a single layer. When the conventional critical height equation was used, the undrained shear strength was estimated to be 48 kPa. Undrained shear strength was then back calculated for the potential (Figure 4) and actual (Figure 5) failure plane considering the tension crack as part of slip surface, which led to 60 and 89 kPa, respectively. The undrained shear strength back calculated assuming slip circle was the same as the one based on the critical height (i.e. 48 kPa). Computations were also performed considering various individual strata properties using the conventional limit equilibrium method as shown in Figure 6. For each stratum, undrained shear strength obtained from laboratory was proportionally revised until factor of safety (FOS) = 1. Summary of various computed undrained strength is presented in Table 1. According to Table 1, the undrained shear strengths obtained based on critical height equation and first potential failure surface are more reasonable compared to that for actual failure plane.

Table 1. Undrained shear strength (between EL.170.8 m and EL. 160 m) used by Kwan (1971) to estimate the stability of unsupported vertical cut extending the total stress approach

Method	Computed average (kPa)
Critical height	48
First potential failure surface (Figure 4)	60
Actual failure plane (Figure 5)	89
Slip circle	48
Conventional test data	38

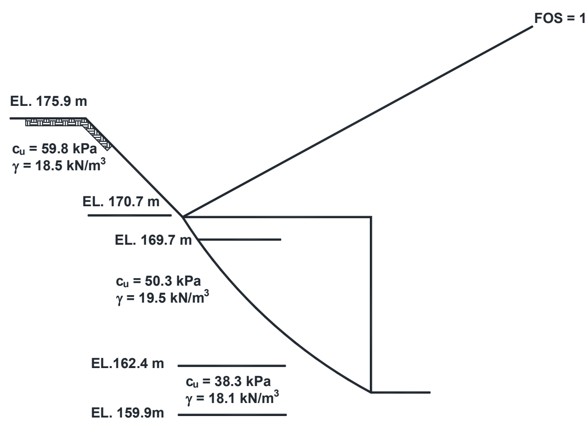

Figure 6. Computed undrained strength of individual stratum (after Kwan 1971)

Effective stress analysis was also carried out using the effective strength parameters obtained from triaxial tests and the equipotential contours of pore-water pressure. FOS of 0.9 and 1.07 were obtained with Bishop's simplified method and conventional method, respectively. This justifies that the failure in unsupported vertical cut was caused by the development of the tension crack. Kwan (1971) mentioned that the application of effective stress analysis is more reasonable since it captures the dissipation of pore pressures throughout the excavation.

4 NUMERICAL ANALYSIS

4.1 Soil Properties

Soil profile was simplified with three different layers; namely, overburden lacustrine silty clay, clayey silt till and lacustrine silty clay from the top. Material properties of each layer were adopted from Kwan (1971) and Banerjee et al. (1988) and summarized in Table 2.

Table 2. Material properties used in the numerical analysis (adopted from Kwan 1971 and Banerjee et al. 1988)

Soil type	Elevation (m)	c' (kPa)	ϕ' (°)	k_{sat}* (m/s)
Lacustrine silty clay	169.7-175.8	9.58	21.5	5×10^{-7}
Clayey silt till	162.4 - 169.7	13.4	24.5	5×10^{-7}
Lacustrine silty clay	157.7 - 162.4	13.4	22.6	5×10^{-8}

* saturated coefficient of permeability

According to Banerjee et al. (1988), the properties of clayey silt were similar to Weald clay (Schofield and Wroth 1968). In addition, the plasticity index and percent passing 425 mm sieve for Weald and London clays are similar as well. Hence, in the present study, the SWCC of London clay was used for the clayey silt layer. In case of the SWCC of Lacustrine silty clay, the SWCC of sample material, 'Silty Clay' available in GeoStudio 2019 R2 was used. The SWCC and hydraulic conductivity functions used in the numerical analyses are shown in Figure 7 and Figure 8 respectively.

4.2 Numerical Analysis

Figure 9 shows mesh and boundary conditions defined in SIGMA/W to conduct finite element analysis. Quadrilateral and triangle mesh with secondary nodes were used to define regions with global size of 0.5 m near the excavated areas based on the sensitivity analysis. Stress/strain boundary conditions were assumed to be restrained in horizontal (X) direction at the vertical ends (i.e. fixed-X displacement boundaries; hollow red triangles) and restrained in both horizontal (X) and vertical (Y) directions at the bottom (i.e. fixed-XY boundaries along the base of the domain). Water total head hydraulic boundary condition which is equal to the elevation of initial water table (i.e. elev. 173.8m) was assigned along the lateral extents of the soil region on the vertical ends. Excavation was simulated by deactivating regions with 'coupled stress-pore pressure' analysis. This analysis type gives both displacement and pore-water pressure changes simultaneously (hereafter referred to as coupled analysis). Once excavation is completed, slope stability analyses was carried out in SLOPE/W based on the SIGMA/W results (i.e. deformation and pore-water pressure due to excavation) as the parent analysis. Among various analysis type in SLOPE/W, "SIGMA/W stress" was chosen for stability analysis with the ‘Entry and Exit’ slip surface option. To maintain the consistency of estimated results with measured field results, excavation was simulated following the same timeline as followed in the field.

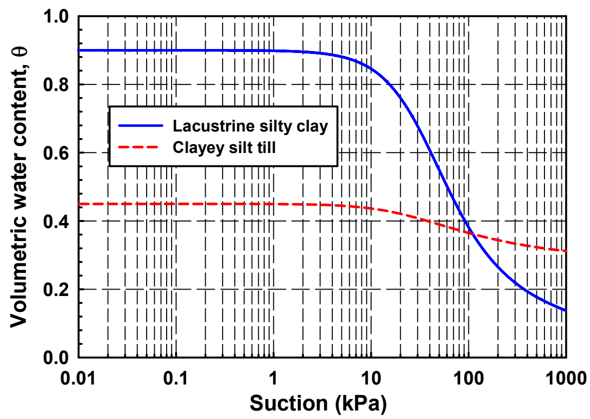

Figure 7. Soil-Water Characteristic Curve for materials used in numerical analysis

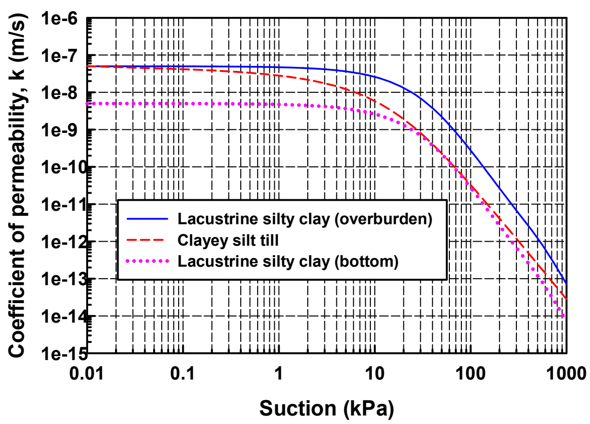

Figure 8. Permeability function for materials used in numerical analysis

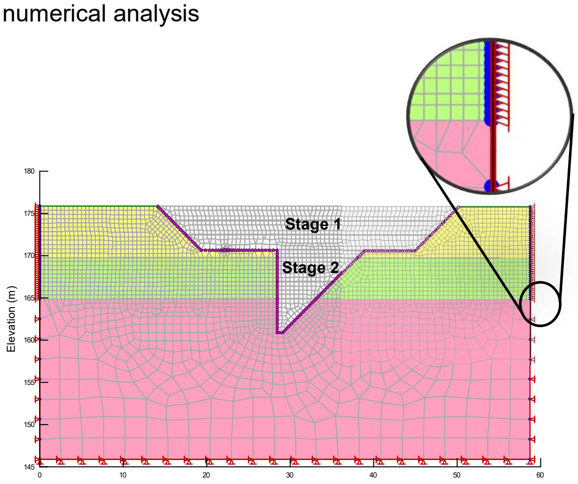

Figure 9. Mesh and boundary conditions used in the numerical analysis (11853 nodes, 4523 elements)

5 RESULTS AND ANALYSIS

A significant drop of pore pressure was observed near the unsupported vertical cut area during excavation. Figure 10 shows the comparisons of measured and estimated (coupled analysis) pore-water pressure contours (0 (i.e. phreatic line), 60, and 120 kPa) 12 days after removal of top sediment layer.

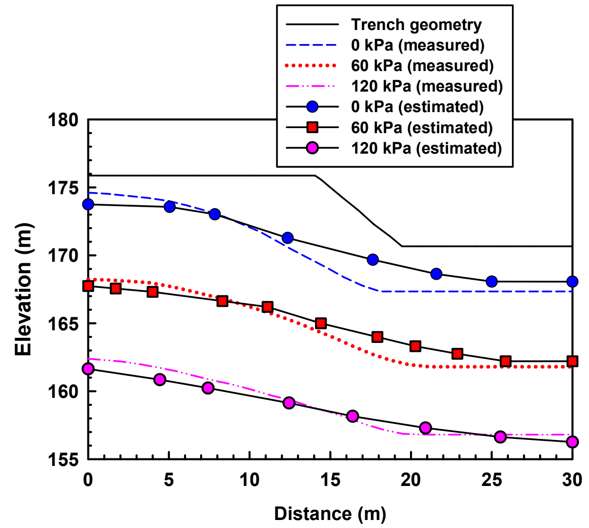

Figure 10. Comparisons of measured and estimated pore-water pressure contours (0 (i.e. phreatic line), 60, and 120 kPa) 12 days after removal of top sediment layer

Comparisons of measured and estimated pore-water pressure contours (0 kPa (i.e. phreatic line) and 60 kPa) after the completion of vertical excavation but prior to failure are shown in Figure 11.

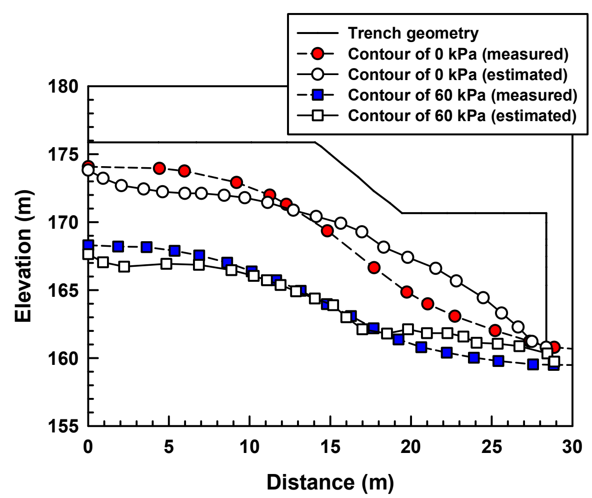

Figure 11. Comparison of measured and estimated pore-water pressure contours (0 (phreatic line) and 60 kPa) prior to failure.

Based on the estimated pore-water pressure, FOS was estimated to be 1.05 as shown in Figure 12.

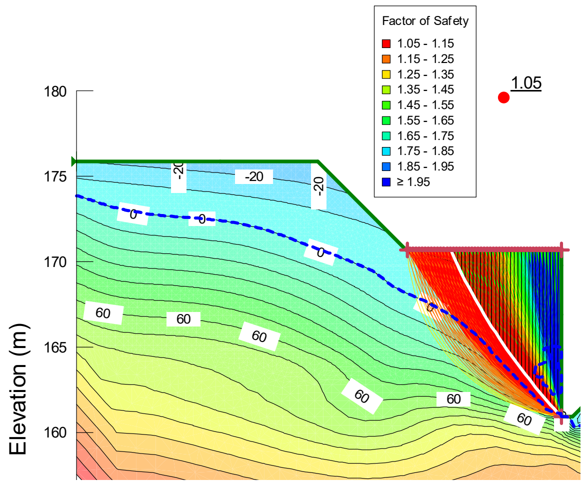

Figure 12. Pore-water pressure distribution and FOS prior to failure without tension crack (coupled - SIGMA/W stress method)

As mentioned in previous section, the failure of unsupported vertical cut occurred under the influence of tension crack. Hence, additional stability analysis was performed by simulating a tension at the berm of the unsupported vertical cut. Tension crack was simulated as a void (0.1 m opening) with zero strength in SIGMA/W. The bottom of tension crack was specified as entry range such that the failure is initiated from the bottom of the tension crack. The exit point was specified at the toe of unsupported vertical cut. With the simulated crack located at 2.43 m from the face of unsupported vertical cut, depth of tension crack was estimated to be 6.55 m with sheared surface inclined at 52 ° to the horizontal (Figure 13). This failure surface was identical to the geometry of the second tension crack and failure surface (actual) observed in field (Figure 5). This analysis results matches the field failure condition. This also confirms the fact that tension crack hinders the stability of slope as it forms a part of slip surface leading towards shortening the length of failure surface (Wang et al. 2012).

6 SUMMARY AND CONCLUSIONS

A series of finite element analysis was performed to simulate the excavation of unsupported vertical cut (depth = 9.75 m) in clay at Welland, Ontario (Kwan 1971). The excavation was simulated following the same timeline as field excavation. There was a good comparison between the post excavation pore-pressure data obtained from installed instruments and those obtained through numerical modelling study. The numerical analysis results showed that the failure in unsupported vertical cut was attributed to a tension crack, which is consistent with field observations.

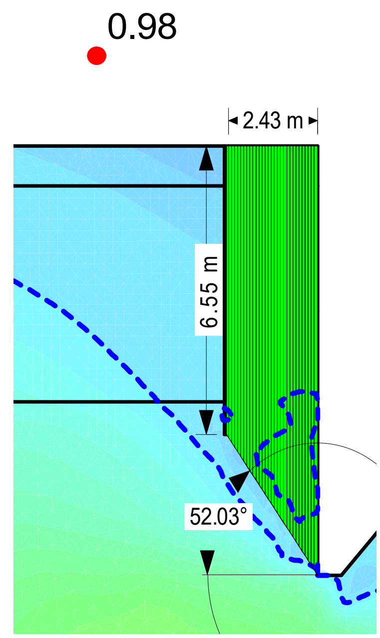

Figure 13. Stability analysis performed replicating the second (actual) tension crack

7 REFERENCES

Banerjee, P.K., Kumbhojkar, A. and Yousif, N.B. 1988. Finite element analysis of the stability of a vertical cut using an anisotropic soil model, *Canadian Geotechnical Journal*, 25(1): 119-127.

Bishop, A.W. and Bjerrum, L. 1960. The relevance of the triaxial test to the solution of stability problems, *ASCE Conference on Strength of Cohesive soils*: 437-501.

DiBagio, E., and Roti, J.A. 1972. Earth pressure measurements on a braced slurry-trench wall in soft clay, *In Proceedings of the 5th European Conference on Soil Mechanics and Foundation Engineering*, 1: 473-484.

Dysli, M., and Fontana. 1982. Deformations around the excavations in clay soil, *In Proceedings of the International Symposium on Numerical Models in Geomechanics*, Zurich, Edited by R. Dunger and J. A, Studer: 634-642.

GEO-SLOPE International, Ltd. 2013. Stability modeling with SLOPE/W, user's guide. *GEO-SLOPE International Ltd.*, Calgary, Canada.

GEO-SLOPE International, Ltd. 2013. Stress-Deformation modeling with SIGMA/W, user's guide. *GEO-SLOPE International Ltd*., Calgary, Canada.

Irvine, D.J., and Smith, R.J.H. 1983. Trenching practice, *CIRIA Report 97*, London.

Kwan, D. 1971. Observation of the failure of a vertical cut in clay at Welland, Ontario, *Canadian Geotechnical Journal*, 8(2): 283-298.

Lambe, W., and Turner, K. 1970. Braced excavations, *Lateral Stresses in the Ground and Design of Earth-Retaining Structures*: 149-218.

Leroueil, S., La Rochelle, P., Tavenas, F., and Roy, M. 1990. Remarks on the stability of temporary cuts, *Canadian Geotechnical Journal*, 27(5): 687-692.

National Bureau of Standards. 1988. Recommended technical provisions for construction practice in shoring and sloping of trenches and excavation, *NBS Building Science Series 127*.

Oh, W.T. and Vanapalli, S.K. 2018. Undrained shear strength of unsaturated soils under zero or low confining pressures in the vadose zone, *Vadose Zone Journal*.

Schofield, A.N. and Wroth, C.P. 1968. Critical state soil mechanics, *McGraw-Hill*, London, England.

Vanapalli, S.K., Fredlund, D.G., Pufahl, D.E. and Clifton, A.W. 1996. Model for the prediction of shear strength with respect to soil suction, *Canadian Geotechnical Journal*, 33(3): 379-392.

Wang, Z.F., Li, J.H. and Zhang, L.M. 2012. Influence of cracks on the stability of a cracked soil slope, *In Proceeding of the 5th Asia-Pacific Conference on Unsaturated Soils*, Pattaya, Thailand, 2: 594-600.